PCCP

On the structure and coordination of the oxygen-donating species in Ti↑MCM-41/TBHP oxidation catalysts: a density functional theory and EXAFS study

Carolyn M. Barker,[a] David Gleeson,[a] Nikolas Kaltsoyannis,[b] C. Richard A. Catlow,[a] Gopinathan Sankar[a] and John Meurig Thomas[a]

[a] *The Davy Faraday Research Laboratory, The Royal Institution of Great Britain, 21 Albemarle Street, London, UK W1S 4BS*
[b] *Department of Chemistry, University College London, 20 Gordon Street, London, UK WC1H 0AJ*

Received 31st May 2001, Accepted 25th October 2001
First published as an Advance Article on the web 4th March 2002

We present a combined density functional theory and EXAFS investigation into the geometry and coordination of the oxygen-donating species in surface grafted, *tert*-butyl hydroperoxide (TBHP) exposed Ti↑MCM-41 oxidation catalysts. The formation of a number of different Ti(η^2-peroxo) and Ti(η^1-peroxo) type species, including radical and anionic complexes, has been examined, arising from the attack of peroxide (where both hydrogen peroxide and TBHP have been studied) on a tetrahedral Ti^{IV} site, together with and without one molecule of water. BP86/DZVP calculations show that the Ti(η^1-OO^{t}Bu) complex is 33 kJ mol^{-1} lower in energy than the Ti(η^2-OO^{t}Bu) complex which is contrary to previous estimates in the literature and we propose that 6-coordinate Ti(η^1-OOR) complexes, where R is the peroxide substituent (*i.e.* R = H for H_2O_2 and R = ^{t}Bu for TBHP), are the oxygen-donating species in peroxide/titanosilicate mixtures. X-ray absorption analysis is in good agreement with our DFT predictions that Ti–peroxo species in TBHP/Ti↑MCM-41 systems are 6-coordinate. Furthermore, our DFT cluster calculations and X-ray absorption analysis collectively reveal the presence of 6-coordinate ' Ti(η^2-OO^{t}Bu)(OHR) ' and ' Ti(η^1-OO^{t}Bu)(OHR)·H_2O ' complexes in TBHP/Ti↑MCM-41 catalysts.

Introduction

Porous titanosilicates continue to attract considerable attention due primarily to their remarkable catalytic efficiency in the oxidation of a wide variety of small-chain hydrocarbons.[1,2] Uniquely, in the presence of an *aqueous* hydroperoxide and at temperatures < 350 K, titanosilicate mediated oxidations typically occur with high target product yields and selectivities and with minimal decomposition of the sacrificial oxidant. Several porous titanosilicate catalysts have been employed for oxidation reactions, ranging from microporous TS-1[3] and Ti-β,[4] to mesoporous Ti-MCM-41.[5,6] The latter has attracted particular interest, since restrictions on substrate size, imposed by the microporous environment of titanosilicates such as TS-1 and Ti-β (pore diameter 4–10 Å), are removed in mesoporous silicas such as Ti-MCM-41 due to their large pore size (~30–100 Å). Furthermore, the synthesis of mesoporous titanosilicates allows for applications in the fine chemical and pharmaceutical industry where bulkier substrates are typically employed.

X-ray absorption,[5–12] infra-red,[7,8,13,14] UV–vis spectroscopy[7,8,15,16] and computational studies[17–22] have collectively revealed that, regardless of synthetic procedure, the tetravalent titanium centres in both microporous and mesoporous titanosilicates are 4-coordinate when in a *dehydrated* medium. However, upon exposure to water, peroxide or other adsorbates, there is evidence that this unsaturated coordination number of 4 increases reversibly to 5 or 6.[23] From X-ray absorption studies alone, we have determined that titanium is present in a distorted octahedral environment.[5,24] However, as we have recently reported,[11] the exact nature of this type of species is still undergoing debate. Cleavage of the Ti–O–Si bonds is known to occur and density functional theory (DFT) calculations[25] have suggested that a mixture of (–SiO)$_4$Ti, (–SiO)$_3$Ti(–OH) and (–SiO)$_2$Ti–(OH)$_2$ sites (species I–III, Fig. 1, respectively) are probable in catalysts where the metal ions have been isomorphously substituted into the framework. In grafted Ti^{IV} silicas, it is improbable that neighbouring silanols would condense to form species I and we have shown, through a combination of EXAFS and DFT, that a mixture of species II and III is probable in titanocene dichloride grafted Ti↑MCM-41.[19]

The nature and coordination of Ti^{IV} sites in porous titanosilicates is an important question to address. However, tetrahedral Ti^{IV} sites alone are not the catalytically active species in oxidations. The mechanism by which titanium substituted molecular sieves facilitate the oxidation of small-chain hydrocarbons, such as the conversion of alkenes to epoxides, has been explained by the formation of oxygen-donating

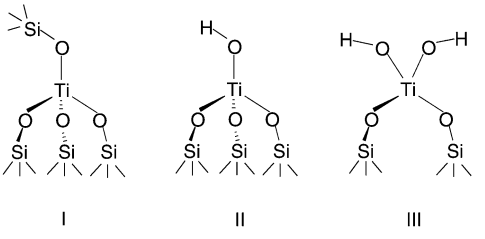

Fig. 1 Proposed models of tetrahedral Ti sites in *dehydrated* porous titanosilicates.[6,7,13,15]

 DOI: 10.1039/b104735n

titanium–peroxo complexes, arising from attack of the hydroperoxide on the metal centres.[26–28] Detailed knowledge of the nature of the Ti–peroxo species formed in titanosilicate/peroxide mixtures is of critical importance if the catalytic mechanism of oxidation transformations is to be fully understood.

In the present paper, we address this problem using a joint computational and experimental approach whose power has been proved[19] in a number of previous studies. Because of the difficulties associated with probing titanosilicates by experimental techniques alone (the Ti ions are randomly located and in a dilute concentration within the silica matrix) there has been much speculation but limited direct evidence regarding the nature of the oxygen-donating species formed within these solids. In the next section we outline the main proposals in the literature to date regarding the structure and coordination of Ti–peroxo complexes in titanium substituted molecular sieves. A number of groups have postulated that in alkene epoxidation reactions the substrate may initially bind to the Ti centre before peroxide interaction.[29,30] However, the calculations of Sinclair and Catlow[28] found no evidence of initial ethene binding to tetrahedral Ti sites in their DFT cluster calculations. Thus, pre-peroxide alkene binding to the tetrahedral Ti sites has not been considered in the present study.

Models for oxygen donating species

In the liquid phase, H_2O_2 is known to act as a strong, bidentate ligand to Ti^{IV} compounds, displacing other substituents to form extremely stable η^2 Ti–peroxo radical species (IV, Fig. 2). Such Ti–peroxo compounds have been suggested as the oxygen-donating species in titanosilicate oxidation catalysts.[26] Indeed, IR,[22,31] UV–vis,[15] EPR[15] and quantum chemical[28,32] studies of titanosilicate/H_2O_2 systems all indicate the presence of η^2-peroxo species. Moreover, DFT calculations by Sinclair[33] have suggested that a characteristic UV–visible absorption band at 26 000 cm^{-1}, observed for TS-1/H_2O_2 systems and attributed to a $O_2^{2-} \rightarrow Ti^{4+}$ charge transfer process,[15] is due to the presence of Ti(η^2-O_2) species. However, Sinclair[33] also postulated that in alkene epoxidation reactions Ti(η^2-O_2) complexes will only form in the absence of the substrate and therefore cannot be the catalytic mediating species.[33] Furthermore, Ti(η^2-O_2) complexes do not explain the observed influence of the nature of peroxide substituents on the reaction kinetics of porous titanosilicate catalysts.[34–36] In addition, it has been reported that TS-1/H_2O_2 mixtures are acidic, whereas TS-1/alkyl peroxide catalysts have no acidic properties.[35,37,38] However since the Ti(η^2-O_2) type complexes derived from *tert*-butyl hydroperoxide (TBHP) or H_2O_2 would be indistinguishable, this type of species cannot explain this apparent change in acidity.

Alkyl hydroperoxides (ROOH) are known[1,39,40] to form both η^2-OOR and η^1-OOR complexes with transition metals (species V, VII, Fig. 2 respectively), depending on the binding strength of other ligands. Transfer of electron density from the partially filled π^* O–O anti-bonding orbitals of the peroxidic oxygen(s) to the Ti^{IV} centre has been proposed[1] to stabilise η^2-OOR species. Indeed, a number of quantum chemical studies have suggested that Ti(η^2-OOR) species are stable[28] and energetically accessible and that they provide an explanation for the previously mentioned peroxide and acid–base effects[22,26,38] observed for titanosilicate/peroxide mixtures.

However, Ti(η^2-peroxo) species do not explain the well-documented dependence on solvents and additives of the catalytic efficiency of titanosilicate/peroxide systems.[26,27,34,36,37,41–43] Thus, many workers champion a Ti(η^1-OOR) complex or a 5-membered ring intermediate[17,27,31,38,44] where the solvent or adsorbate is an integral part of the compound, offering stabilisation of the peroxide moiety through hydrogen bonding (species VII and VIII, Fig. 2). Furthermore, species VII and VIII also have several organic analogues.[45] However, it is important to note that TS-1 is active for alkene epoxidations in the absence of solvents (although with reduced activity)[35] and species VII and VIII would, therefore, not be essential for this mode of reaction. In addition, quantum mechanical simulations of small model $Ti(OH)_4$ clusters found the Ti(η^1-OOH) complex to be 33 kJ mol^{-1} less stable than the Ti(η^2-OOH) complex.[30]

To solve the problem of the structure of these crucial intermediates, we have undertaken a combined DFT and EXAFS investigation into the geometry, coordination and stability of Ti–peroxo complexes in porous titanosilicate/peroxide mixtures. Firstly, we discuss the stability of Ti(η^2-peroxo) and Ti(η^1-peroxo) complexes with respect to the catalytic reactants, a tetrahedral (–SiO_3)TiOH complex (species II, Fig. 1) and a hydroperoxide (hydrogen peroxide and TBHP will both be examined), both with and without one molecule of water. In addition, we present evidence for a new, stable Ti–peroxo species. We show that analysis of Ti K-edge X-ray adsorption spectra of a TBHP exposed Ti↑MCM41 catalyst is in good agreement with our DFT predictions concerning the likely nature of Ti–peroxo species. Our calculations strongly indicate that the formation of bidentate ' ≡Ti–η^2(O_2) ' complexes is highly endothermic (> 400 kJ mol^{-1}) but that the formation of 6-coordinate Ti(η^1-OOR) and Ti(η^2-OOR) species, where R is the peroxide substituent, is exothermic. Such models accord well with the experimental EXAFS data.

Computational methodology

Gradient corrected (DFT) as embodied in the code Dgauss[4.1,46] part of the UniChem[4.1] package,[47] was used for the majority of the geometry and energy calculations. Owing to the computationally demanding nature of DFT calculations, a finite molecular cluster approximation was employed, where the catalytically active site was represented in the majority of the calculations by a tetrahedral $(H_3SiO)_3$Ti–OH cluster, which extends two coordination spheres from the central titanium cation although in a limited number of cases larger clusters were employed as discussed below. As we have previously noted for a dehydrated Ti^{IV}–silica generated by a

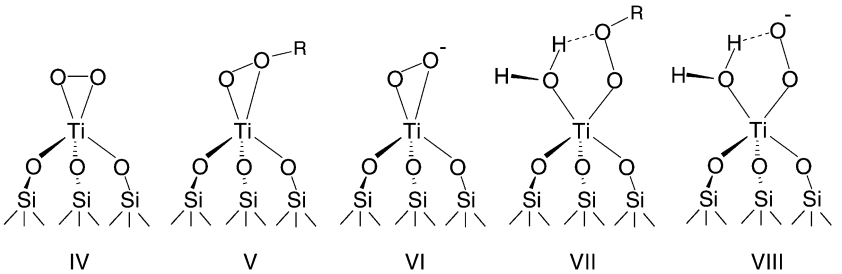

Fig. 2 Literature postulated models for Ti–peroxo species in dehydrated, porous titanosilicate/hydroperoxide catalysts.[1,28,31,32,37,38,45] R = H or ^{t}Bu when ROOH = H_2O_2 or TBHP.

grafting procedure, only Ti–OH and $Ti(OH)_2$ sites are thought likely to exist. In this study, we have chosen to examine the attack of peroxide on only the tripodal Ti–OH, type complex, species II (Fig. 1). A more complete treatment of titanosilicates would naturally take into account the steric, polarising and electrostatic effect of the molecular sieve lattice. However, finite clusters have been found to provide a good approximation for this system,[17,28,48] since reactivity is localised around the dilute Ti sites.

The initial geometry of the Ti–OH cluster was taken from our previous work, the protocol and Cartesian coordinates for which are outlined in ref. 28. Partial optimisation of the tripodal Ti^{IV} cluster was then performed employing the gradient corrected functional of Becke[49] and Perdew and Wang[50] (BP86), in addition to the local parameterisation of Vosko and co-workers.[51,52] An all electron double ξ basis with polarisation on all non-hydrogen atoms (DZVP), specifically optimised for DFT, was used throughout. All Si ions were fixed, to represent the rigidity of the silica framework. As discussed in ref. 17, this procedure may over-constrain the cluster, although it is almost certainly a better approximation than allowing complete relaxation of the cluster. The good agreement between the calculated and experimental geometries found in the present paper suggests that for present applications the approximation is acceptable. The resultant optimised initial cluster is pictured in Fig. 3 (species IX). All further clusters which extend two coordination spheres (2 C.S.) from the central metal atom discussed in this work were constructed from species IX, Fig. 3, and were optimised employing the BP86/DZVP procedure and with the Si atoms constrained at their original positions. The molecular cluster approximation used here clearly has limitations; future work will be needed to employ embedded cluster techniques. For the calculation of local geometries—the main purpose of this paper—in zeolite materials, the method is, however, effective and adequate.

EXAFS spectroscopy probes the local structure around the Ti centres and is accurate for the first and second coordination shell. However, as noted, the Si ions within the second coordination shell were fixed in conformational space during computational optimisation. Thus, in order to allow full relaxation of the first two shells, which are compared with experiment, selected Ti–peroxo clusters, which are presented in the Results and discussion section, were also calculated employing a larger model cluster, extending 3 coordination spheres from the central Ti ion. The DFT code Dmol,[53] available as part of the Cerius[2] (version 4.2) suite,[54] was used for all geometry and energy calculations of the extended or 3 C.S. clusters (species X, Fig. 3). This code was chosen owing to its efficiency in treating large molecular systems. The Becke exchange[49] and the Perdew and Wang correlation gradient corrections[50] to the functional of Vosko and co-workers [51,52] were again employed for all geometry optimisations and energy calculations, coupled with an all-electron, double numeric basis with polarisation on all non-hydrogen atoms, DNP. The initial 3 C.S. cluster was cut from a standard silicalite (MFI zeolite type) model available within MSI's Cerius[2] library, with all severed bonds capped by hydrogen atoms. The purely siliceous starting model was optimised using the BP86/DNP DFT method, keeping the outermost oxygen ions fixed in conformational space. The central, tetravalent Si ion in the minimised silicalite model was replaced with Ti and the resultant complex re-optimised. Geometrical constraints were imposed upon the Cartesian coordinates of the outer oxygen ions.

No symmetry constraints were used throughout this work and all optimisations were performed in Cartesian coordinates. A spin unrestricted wave function was employed in modelling the Ti–(η^2-O_2) and H_3O radical species. The maximum deviation from the ideal expectation value of the spin quantum number (*i.e.* $\langle S^2 \rangle$) was 0.0046, indicating minimal spin contamination when employing the spin unrestricted wave function.

Experimental methodology

Ti K-edge XAS data were collected at station 8.1 of the Daresbury Synchrotron radiation source, which operates at 2 GeV with a typical ring current of 150–250 mA. This experimental station is equipped with a Si(111) monochromator, ion chambers for the measurements of incident and transmitted beam intensities and a 13 element Canberra detector for measurement in fluorescence mode. Since the majority of the catalyst samples contained less than 2 wt.% of titanium centres, all EXAFS measurements were performed in fluorescence mode. The transmission mode was utilised for the standards in order to avoid self-absorption effects. XAS measurements of dehydrated samples were performed in an *in situ* cell, which is described in detail elsewhere.[55] In a typical experiment *ca.* 100 mg of the catalyst were pressed into a 20 mm disc and loaded into the *in situ* cell. The sample was heated in an oxygen atmosphere to 500 °C for 1 h, and subsequently cooled to room temperature prior to the XAS measurement. In a separate experiment, a dehydrated Ti (2%)-MCM-41 catalyst was reacted with TBHP for 1 h. Notably, the sample turned yellow, a characteristic of active peroxide/titanosilicate mixtures. EXAFS data of the active catalyst were measured at room temperature. Energy calibration was conducted with a 5 μm thick titanium foil. The second monochromator was de-tuned to achieve a 50% harmonic rejection. At least 4 scans for each sample were carried out and summation of the data was performed to yield the best signal : noise ratio.

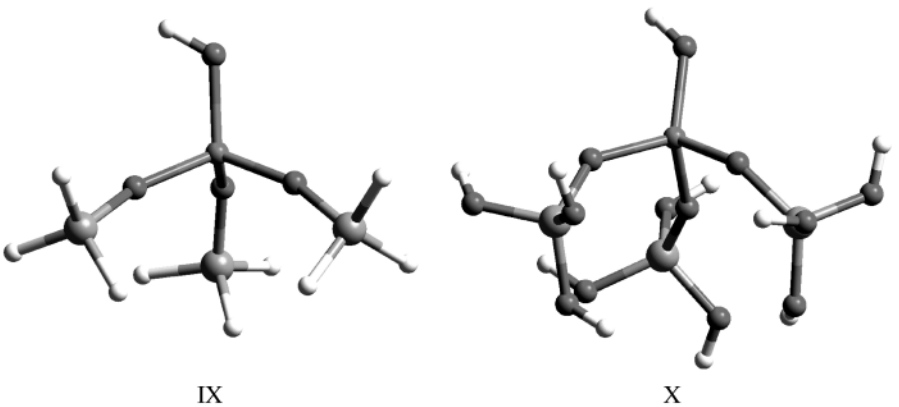

IX X

Fig. 3 (a) BP86/DZVP (DGauss) optimised tripodal $(H_3SiO)_3Ti$–OH cluster, (b) BP86/DNP (DMol) optimised tripodal, extended TiOH cluster.

Data analysis

The Ti K-edge EXAFS data were processed using the EXCALIB, EXBROOK and EXCURV suite of programs, available at the Daresbury Laboratory. EXCALIB and EXBROOK are employed to convert the data from intensities and monochromator angle to energy *versus* absorption and to carry out background subtraction for production of the final EXAFS spectra respectively. In addition, EXBROOK is used to normalise the data in order to produce the XANES part of the XAS. EXCURV(98) was employed to carry out the refinement procedure to obtain the best fit between experimental and calculated EXAFS. Within the EXCURV program, all the non-structural parameters, in particular the phase shifts associated with the various atoms, were calculated prior to the detailed curve fitted analysis. In this work we have employed a multiple scattering procedure we developed previously.[11] In a typical analysis of the EXAFS data, we employed each of the DFT energy minimised clusters as the starting geometrical configurations for refinement, including all atomic coordinates. Initially the EXAFS data were fitted to a model consisting of the first coordination sphere of oxygens. The values of the Ti–O distances, the Debye–Waller factors and of E_o were refined to yield the best fit. The EXAFS data were then fitted to the full cluster derived from the DFT calculations. C_1 symmetry was used throughout as higher symmetries could not describe the models. In order to avoid correlation effects, the Ti–O distances and the Debye–Waller factors of the Ti–O–Si linkages were constrained to be equal. Additionally, it was necessary to fix the O–Si distance at a typical distance of *ca.* 1.6 Å, and the O–O distance of the peroxo species to *ca.* 1.45 Å. For the refinement of the Ti–Si and Ti–peroxo oxygen species, the individual distances and bond angles were allowed to vary freely whilst the Debye–Waller factors of closely similar bond distances were constrained to be equal. These constraints produced no unphysical results and indeed have been shown previously[11] to control the refinement in such a way that some of the correlations are minimised to produce results that are consistent with crystallographic data.

Results and discussion

Firstly, we will present the results of our DFT calculations concerning the geometries and energies of 5- and 6-coordinate Ti(η^2-peroxo) complexes, (IV–VI, Fig. 2). Attention will then focus on our quantum chemical treatment of the previously postulated Ti(η^1-peroxo) compounds (VII and VIII, Fig. 2), again with regard to their geometrical configuration, coordination and energy. We will then discuss the finding of an additional, stable, Ti(η^1-peroxo) identified for the first time in this work. Analysis of Ti K-edge EXAFS data of TBHP exposed Ti↑MCM41 will then follow, employing the DFT calculated clusters as starting models for the experimental refinement.

DFT calculated Ti(η^2-peroxo) species

We have already noted that three alternative η^2 Ti–peroxo configurations have been proposed as representations of the oxygen-donating species in porous titanosilicate systems: a Ti–alkyl peroxide, its anionic analogue and a Ti–peroxo radical complex (V, VI and IV, Fig. 2, respectively). The latter form is known to have remarkable stability in the liquid-phase. For computational rapidity, we have in most of our calculations modelled hydrogen peroxide as the sacrificial oxidant. Since the EXAFS data were collected using TBHP as the oxidant, calculations on selected configurations were subsequently repeated employing this ligand, which we found has little effect on the local geometry of the Ti species.

We have calculated optimised geometries of 6- and 5-coordinate (*i.e.* hydrated and dehydrated) η^2 complexes (species IV–VI, Fig. 2) arising from the reaction of hydrogen peroxide with the (H_3SiO_3)Ti–OH cluster (species IX, Fig. 3). These transformations are outlined in reactions 1–6, below. The results of the calculations are reported in Table 1. Firstly, examination of reaction 1, shows that formation of the hydrated or 6-coordinate Ti(η^2-OOH) complex occurs by the attack of the peroxide on the tetrahedral titanium centre with subsequent proton transfer from the peroxide to the hydroxyl ligand. This reaction scheme accords with our previous work.[28]

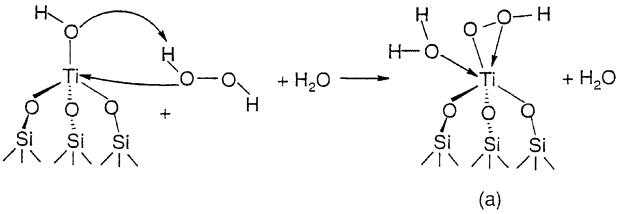

1 'Ti-OH' + H_2O_2 + H_2O → 'Ti(η^2-OOH) · H_2O' + H_2O

Using this scheme but removing the weakly coordinated water ligand, formed by peroxidic proton transfer, allows us to model the formation of the dehydrated or 5-coordinate Ti(η^2-OOH) analogue (reaction 2, Table 1).

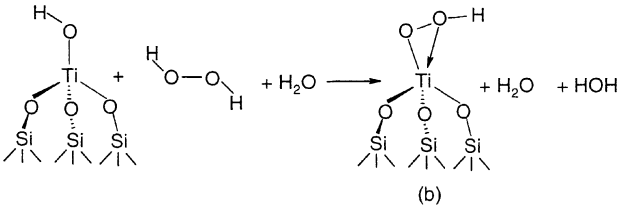

2 'Ti-OH' + H_2O_2 + H_2O → 'Ti(η^2-OOH)' + 2H_2O

We have implemented a similar methodology in order to model the formation of hydrated and dehydrated Ti(η^2-OO^-) clusters (reactions 3 and 4, Table 1), the only difference being that the remaining peroxidic proton is bound to a water molecule to form an H_3O^+ cation.

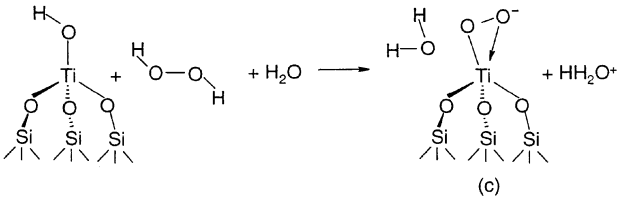

3 'Ti-OH' + H_2O_2 + H_2O → '(η^2-OO^-)' + H_2O + H_3O^+

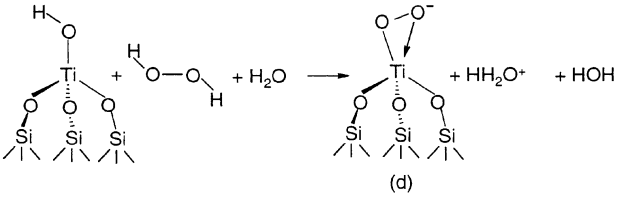

4 'Ti-OH' + H_2O_2 + H_2O → 'Ti(η^2-OO^-)' + H_2O + H_3O^+

Finally, we have adapted reactions 3 and 4 so as to model the formation of the hydrated and dehydrated Ti(η^2-O_2) type radical clusters (reactions 5 and 6, Table 1). We note that reaction schemes 5 and 6, where an $H_3O^{\bullet}$ radical is created, are unlikely to be an accurate representation of the formation of Ti(η^2-O_2) clusters within titanosilicates.

Table 1 BP86/DZVP calculated (in bold) and refined TBHP/Ti↑MCM-41 EXAFS parameters for model 5- and 6-coordinate Ti–η^2(peroxo) species as proposed in the literature. $E_{formation} = E_{total}$(Ti–$\eta^2$(peroxo) + other products) − E_{total}(tripodal Ti^{IV} cluster + H_2O_2 + H_2O). [si] Ti–OSi bond length. [w] The Ti–O bond distance measured is that of Ti to the O in the water molecule. [p] Ti–peroxide bond length

	Hydrated								Dehydrated							
Cluster	Ti–O distance/Å		Ti–Si distance/Å		Ti–O–Si (Ti–O–OH) angle/°		$E_{formation}$/kJ mol^{-1} (*R* factor)		Ti–O distance/Å		Ti–Si distance/Å		Ti–O–Si (Ti–O–OH) angle/°		$E_{formation}$/kJ mol^{-1} (*R* factor)	
Ti–η^2(OOH)	**1.95**[p]	1.91	**3.33**	3.24	**142.9**	141	**−44**		**1.88**[p]	1.86	**3.29**	3.24	**140.4**	140	**−19**	
	2.22[p]	2.19	**3.35**	3.33	**145.7**	151	(15.89)		**2.25**[p]	2.26	**3.43**	3.29	**160.5**	161	(25.2)	
(a)	**1.83**[si]	1.84	**3.45**	3.39	**162.5**	161		(b)	**1.83**[si]	1.84	**3.43**	3.37	**159.4**	157		
	1.84[si]	1.84			**(79.3)**	(83)			**1.81**[si]	1.84			**(82.7)**	(83)		
	1.82[si]	1.84							**1.81**[si]	1.84						
	2.41[w]	2.43														
Ti–η^2(OO^-)	**1.89**[p]	1.85	**3.26**	3.21	**135.2**	137	**+547**		**1.86**[p]	1.87	**3.25**	3.22	**135.4**	136	**+591**	
	1.87[p]	1.85	**3.37**	3.32	**145.3**	149	(26.9)		**1.87**[p]	1.87	**3.42**	3.40	**148.3**	148	(27.8)	
(c)	**1.87**[si]	1.85	**3.44**	3.42	**146.6**	153			**1.87**[si]	1.83	**3.50**	3.45	**160.8**	156		
	1.88[si]	1.81			**(65.8)**	(67)		(d)	**1.92**[si]	1.83			**(66.8)**	(67)		
	1.95[si]	1.91							**1.92**[si]	1.83						
	3.43[w]	3.25														
Ti–η^2(OO)	**2.09**[p]	2.25	**3.32**	3.33	**144.1**	160	**+357**		**2.04**[p]	2.16	**3.43**	3.32	**158.7**	138	**+404**	
	2.04[p]	2.03	**3.27**	3.20	**138.2**	140	(19.3)		**2.03**[p]	1.90	**3.26**	3.33	**138.4**	149	(19.1)	
(e)	**1.80**[si]	1.85	**3.36**	3.41	**142.7**	150			**1.82**[si]	1.86	**3.40**	3.41	**154.3**	161		
	1.82[si]	1.85			**(69.2)**	(82)		(f)	**1.80**[si]	1.86			**(70.4)**	(81)		
	1.87[si]	1.85							**1.81**[si]	1.86						
	2.39[w]	2.39														

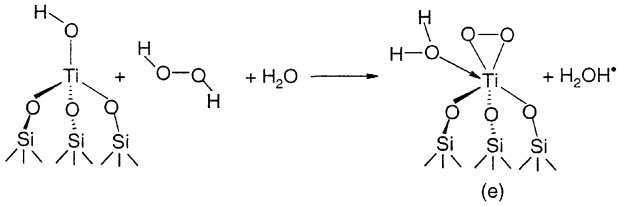

5 'Ti-OH' + H_2O_2 + H_2O → 'Ti(η^2-O_2) + H_2O' + $H_3O^{\bullet}$

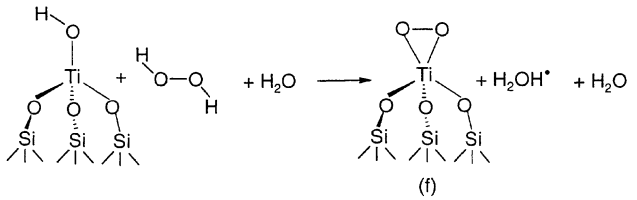

6 'Ti-OH' + H_2O_2 + H_2O → 'Ti(η^2-O_2)' + H_2O + $H_3O^{\bullet}$

However, in order to compare the energy of formation of all Ti(η^2-peroxo) type complexes considered, with each other and with the reactants, these reactions are a convenient way of expressing the evolution of hydrated and dehydrated Ti(η^2-O_2) clusters, respectively. The BP86/DZVP optimised geometries of all 5- and 6-coordinate Ti(η^2-peroxo) complexes and energies of formation as calculated in accordance with reactions 1–6 are shown in Fig. 4 (species a–f respectively). It should be noted that calculation of all Ti clusters was performed in vacuum, *i.e.* with separate computations of the H_2O, H_2O_2, H_3O^+ and H_3O molecules. Thus, all formation energies were calculated using the following equation:

$$E_{formation} = (E_{Ti\text{–}peroxo} + E_{other\ products}) - (E_{TiOH} + E_{H_2O_2} + E_{H_2O})$$

In accordance with the widely accepted proposal that tetrahedral Ti sites reversibly expand their coordination to 6 when in a hydrated media, Fig. 4 shows that for all Ti(η^2-peroxo) type clusters considered, the 6-coordinate metal–peroxo complexes are more stable than their 5-coordinate counterparts. The mode of coordination does not significantly influence the geometrical configuration of the Ti–peroxo fragment, with the water ligand only weakly bound to the metal centre: 25, 45 and 46 kJ mol^{-1} for species a, c and e, respectively. The magnitude of the observed binding energy of water to all the Ti–(η^2-peroxo) clusters studied is consistent with physisorption. Our findings are in good agreement with recent calculations by Sauer *et al.*, who estimated the binding energy of H_2O to tetrahedral Ti^{IV} sites in TS-1 (in the absence of peroxide) to be between 0 and 31 kJ mol^{-1}.[23]

Fig. 4 shows that, regardless of the titanium coordination number, the DFT calculated Ti(η^2-O_2) and Ti(η^2-OO^-) clusters are >300 kJ mol^{-1} higher in energy than their respective reactants, (a TiOH cluster, H_2O_2 and H_2O) and are thus, highly unlikely to form under the mild reaction conditions typically employed for catalytic oxidations. The significance of this observation is that Ti(η^2-O_2) species are known to be extremely stable in the liquid-phase. However, the DFT calculated Ti(η^2-OOH) metal–hydroperoxide cluster is found to be more stable than its respective reactants: −19 kJ mol^{-1} for the 5-coordinate Ti(η^2-OOH) species and −44 kJ mol^{-1} for the 6-coordinate analogue.

To summarise, our DFT cluster calculations suggest that Ti(η^2-OOH) complexes may form in the pores of hydrogen peroxide exposed titanosilicates, with a preferential coordination mode of 6. Conversely, Ti(η^2-O_2) and Ti(η^2-OO^-) type complexes are unlikely to be present, given formation energies of +404 and +357 kJ mol^{-1} for 5- and 6-coordinate Ti(η^2-O_2) radical complexes and +591 and +547 kJ mol^{-1} for 5- and 6-coordinate Ti(η^2-OO^-) compounds respectively. The mechanism and energetics, including activation barriers, of reactions 1–6 will be discussed in more detail in a separate publication.

DFT calculated Ti(η^1-peroxo) species

We have calculated BP86/DZVP optimised geometries for the formation of the five-membered ring or Ti(η^1-OOH) complex (VII, Fig. 2), first proposed by Clerici in 1991,[27] and its anionic analogue (VIII, Fig. 2), outlined in reactions 7 and 8 and 9 and 10.

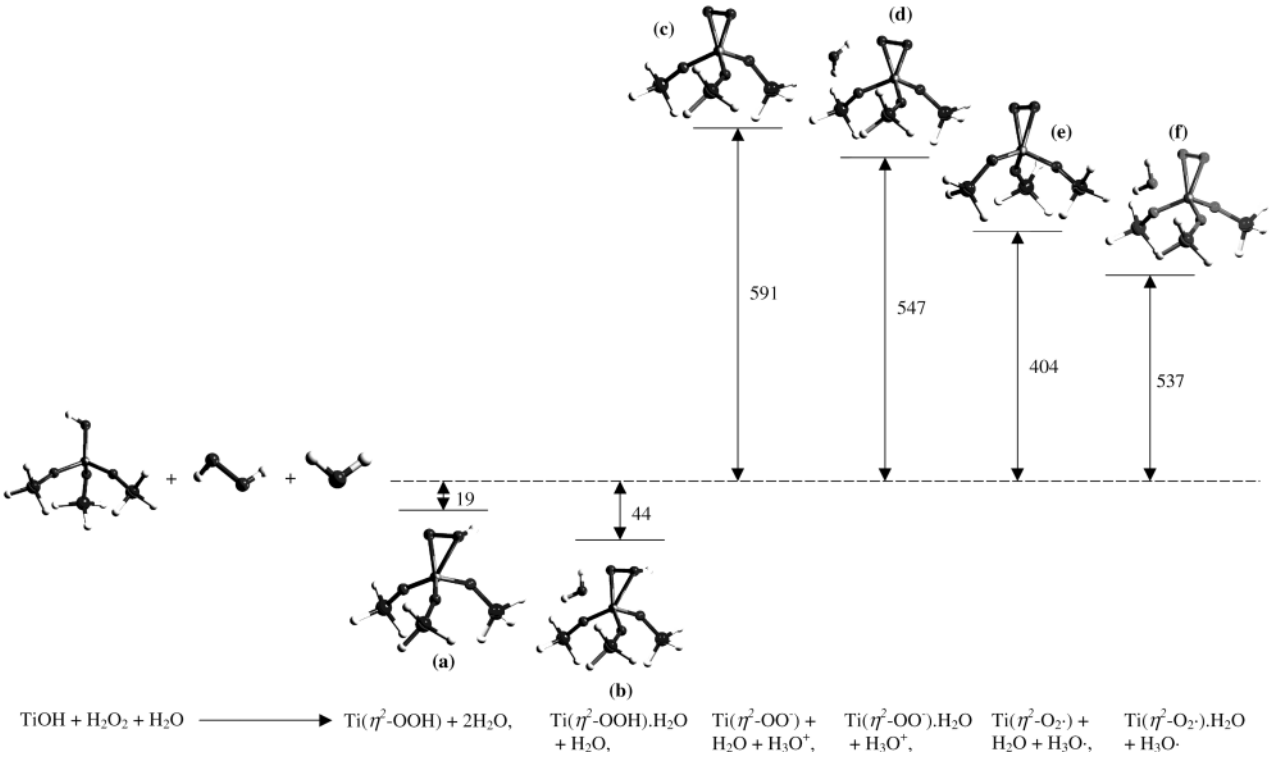

Fig. 4 BP86/DZVP Optimised geometries and energies of formation of 5 and 6 coordinate Ti(η^2-peroxo) species, with respect to the reactants, a tetrahedral Ti site, one molecule of H_2O_2 and H_2O. Energies are shown in kJ mol^{-1}.

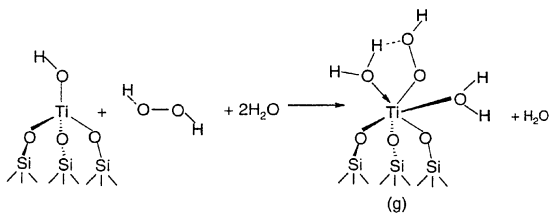

7 'Ti-OH' + H_2O_2 + $2H_2O$ → 'Ti(η^1-OOH)(O(H)H) · H_2O' + H_2O

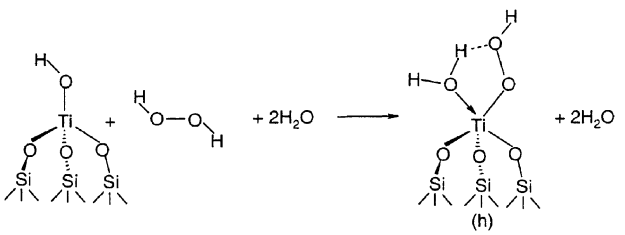

8 'Ti-OH' + H_2O_2 + $2H_2O$ → 'Ti(η^1-OOH)(O(H)H)' + $2H_2O$

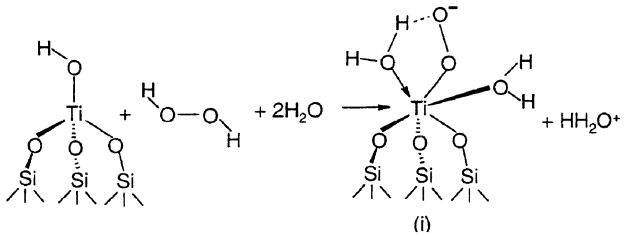

9 'Ti-OH' + H_2O_2 + $2H_2O$ → 'Ti(η^1-OO^-)(O(H)H) · H_2O' + H_3O^+

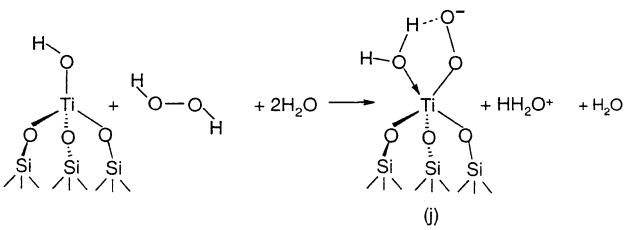

10 'Ti-OH' + H_2O_2 + $2H_2O$ → 'Ti(η^1-OO^-)(O(H)H)' + H_3O^+ + H_2O

The formation of 5- and 6-coordinate Ti(η^1-OOH) and Ti(η^1-OO^-) species again arises from the attack of the peroxide on the metal centre with subsequent proton transfer from the peroxide to the hydroxyl ligand. The resultant five-membered ring configuration is stabilised by hydrogen bonding between the hydroxyl ligand and the peroxo moiety. For the 5- and 6-coordinate Ti(η^1-OO^-) complexes the remaining peroxidic proton binds to a single molecule of water to form an H_3O^+ counter cation.

Fig. 5 shows the BP86/DZVP optimised geometries and calculated formation energies of 5- and 6-coordinate Ti(η^1-OOH) and Ti(η^1-OO^-) clusters, relative to their respective reactants, *i.e.* a tetrahedral site, hydrogen peroxide and water and in accordance with schemes 7–10. Again, all calculations of the Ti clusters were performed in the absence of H_2O and H_2O_2 with minimisation of these molecules performed separately.

Fig. 5 clearly shows that hydration of both the Ti(η^1-peroxo) type clusters is an exothermic process, with the binding energies of one molecule of water to the metal centre (species h and j) calculated to be −24 and −37 kJ mol^{-1} respectively. Thus, in accordance with our studies of Ti(η^2-peroxo) type clusters, 6-coordination is energetically favoured over the unsaturated state of 5 for both Ti(η^1-peroxo) complexes considered. Minimal distortion of the original cluster geometry was observed upon hydration of the 5-coordinate models.

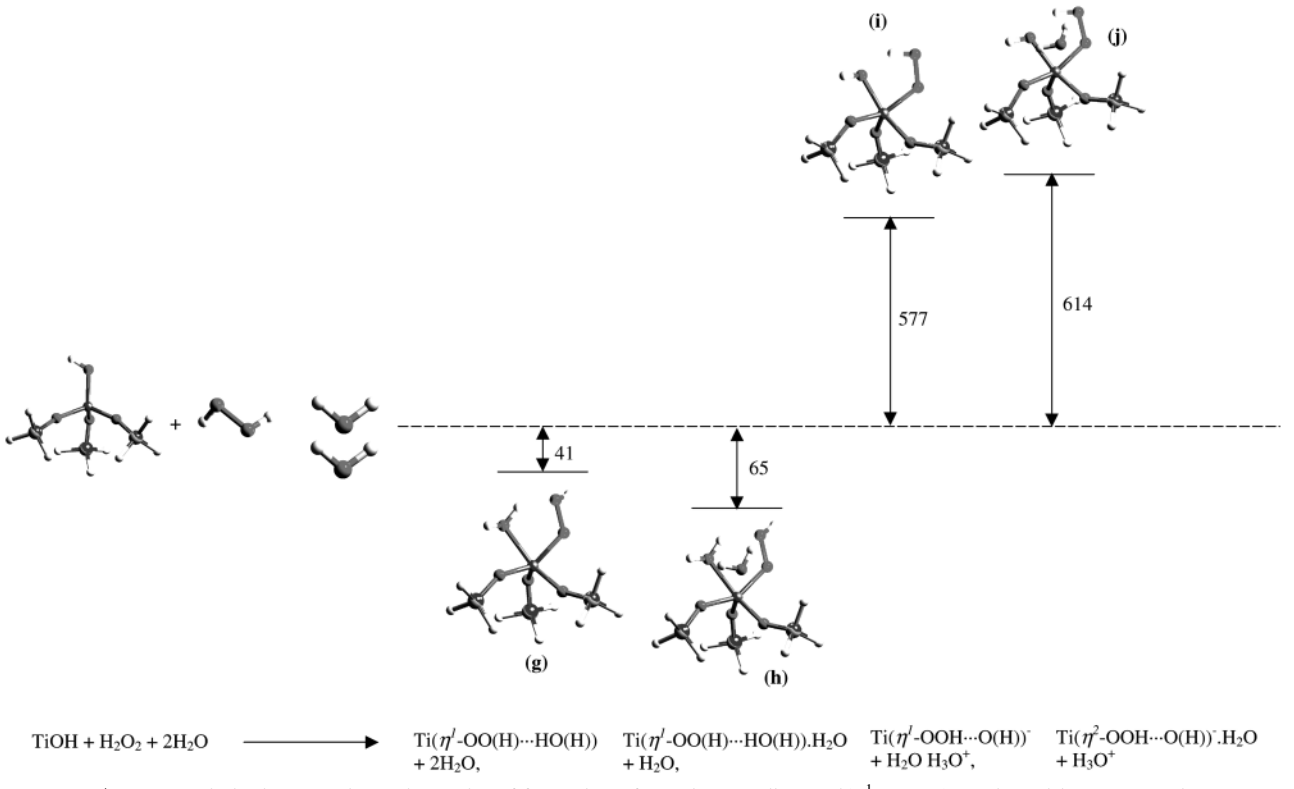

Fig. 5 BP86/DZVP Optimised geometries and energies of formation of 5 and 6 coordinate Ti(η^1-peroxo) species, with respect to the reactants, a tetrahedral Ti site, one molecule of H_2O_2 and two molecules of H_2O. All energies shown are in kJ mol^{-1}.

Furthermore, examination of Fig. 5 shows that the formation of the anionic analogue of the five-membered ring configuration (species j) is again highly unfavourable, +577 and +614 kJ mol^{-1} for 5- and 6-coordination respectively. However, both the 5- and 6-coordinate, Ti(η^1-OOH) species are calculated to be more stable than their respective reactants, −41 and −65 kJ mol^{-1} respectively.

Thus, our DFT calculations suggest that Ti(η^1-OOH) species are likely to be stable within H_2O_2/titanosilicate systems, with formation energies of −41 and −65 kJ mol^{-1} for the 5- and 6-coordinate clusters respectively, relative to a tetrahedral Ti site and one molecule of H_2O_2 and H_2O. Thus, we predict that Ti(η^1-OOH) complexes will preferentially adopt 6-coordination under the mild reaction conditions employed for oxidation catalysis.

Next, we examined the effect of proton transfer on our two predicted models of the Ti–peroxo species in porous titanosilicates (species a and g, Fig. 4 and 5), by transferring the peroxidic proton to the adjacent peroxidic oxygen and re-optimising the resultant cluster. Peroxidic proton transfer of species b and subsequent optimisation resulted in the rotation of the peroxidic moiety (the –OOH fragment) to regenerate the original Ti(η^2-OOH) cluster. However, transfer of the peroxidic proton of species g to the adjacent peroxidic oxygen and optimisation of the resultant geometry resulted in a new, stable Ti(η^1-peroxo) type complex which we shall denote Ti(η^1-O_2H_2). Both the dehydrated and hydrated Ti(η^1-O_2H_2) complexes are presented schematically in Fig. 6 (species k and l, respectively, Fig. 6).

Species k and l (Fig. 6) are formed through monodentate or η^1 binding of the peroxide molecule to the titanium centre with hydrogen bonding between the hydroxyl ligand and a peroxidic hydrogen. Interestingly, our calculations on the hydrated Ti^{IV}(η^1-O_2H_2) cluster resulted in the H_2O molecule preferentially bonding to the peroxide and hydroxy groups, *via* two weak hydrogen bonds rather than coordinating directly to

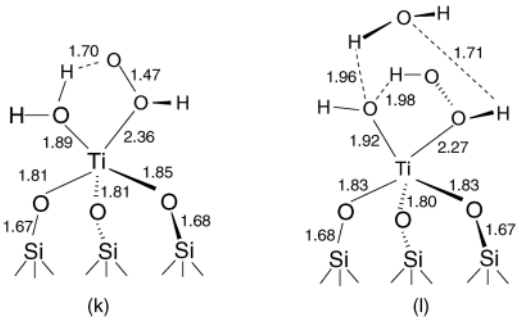

Fig. 6 (**k**) Schematic of the Ti(η^1-O_2H_2) complex isolated by this work. (**I**) hydrated analogue of species XI.

the metal centre (species l, Fig. 6). However, formation of both the dehydrated and hydrated Ti(η^1-O_2H_2) clusters from the attack of H_2O_2 on a tetrahedral Ti centre is calculated to be an exothermic process, −42 and −87 kJ mol^{-1} for species k and l respectively.

Thus, our DFT calculations show that the formation of the previously proposed Ti(η^2-OOH) and Ti(η^1-OOH) complexes and the Ti(η^1-O_2H_2) cluster, proposed in this work, is energetically favourable and that all preferentially exist in a hydrated form, *i.e.* with one water molecule weakly bound to the Ti centre for species Ti(η^2-OOH) and Ti(η^1-OOH) resulting in 6-coordination and for the latter with the water molecule hydrogen bonded to the hydroxyl/peroxide fragment. The energies of formation for the hydrated Ti(η^2-OOH), Ti(η^1-OOH) and Ti(η^1-O_2H_2) complexes with respect to a tetrahedral Ti site, one molecule of H_2O_2 and one molecule of water are −44, −65 and −87 kJ mol^{-1}, respectively.

As we have previously remarked, hydrolysis of the Ti–O–Si bonds in tetrahedral Ti centres (Fig. 1) is known to occur. Furthermore, it is probable that the hydroxyl ligands in

Table 2 BP86/DZVP calculated (in bold) and refined TBHP/Ti↑MCM-41 EXAFS parameters for model 5- and 6-coordinate Ti–η^1(peroxo) species as proposed in the literature. $E_{formation} = E_{total}$(Ti–$\eta^1$(peroxo) + other products) – E_{total}(tripodal Ti^{IV} cluster + H_2O_2 + H_2O). [si] Ti–OSi bond length. [w] The Ti–O bond distance measured is that of Ti to the O in the water molecule. [p] Ti–peroxide bond length

	Hydrated								Dehydrated							
Cluster	Ti–O distance/Å		Ti–Si distance/Å		Ti–O–Si (Ti–O–OH) angle/°		$E_{formation}$/kJ mol^{-1} (*R* factor)		Ti–O distance/Å		Ti–Si distance/Å		Ti–O–Si (Ti–O–OH) angle/°		$E_{formation}$/kJ mol^{-1} (*R* factor)	
Ti–η^1(OOH)	**2.24**	2.21	**3.37**	3.26	**148.4**	156	**−65**		**2.18**	2.19	**3.39**	3.37	**151.3**	161	**−41**	
	1.97[p]	1.99	**3.39**	3.39	**145.5**	142	(15.75)		**1.96**[p]	1.92	**3.42**	3.40	**150.8**	156	(21.37)	
(g)	**1.83**[si]	1.84[si]	**3.39**	3.38	**153.8**	161		(h)	**1.82**[si]	1.84[si]	**3.32**	3.25	**143.9**	141		
	1.89[si]	1.84[si]			**(117.7)**	(117)			**1.86**[si]	1.84[si]			**(122.0)**	(125)		
	1.82[si]	1.84[si]							**1.81**[si]	1.84[si]						
	2.35[w]	2.44														
Ti–η^1(OO^-)	**1.97**	2.22	**3.35**	3.25	**142.2**		**+614**		**1.95**	2.17	**3.40**	3.27	**145.3**	140	**+577**	
	1.92[p]	1.99	**3.41**	3.35	**143.1**				**1.91**[p]	1.82	**3.37**	3.18	**140.7**	132	(21.43)	
(i)	**1.89**[si]	1.85	**3.42**	3.40	**154.6**			(j)	**1.92**[si]	1.89[si]	**3.41**	3.38	**152.0**	161		
	1.95[si]	1.85							**1.94**[si]	1.89[si]			**(122.0)**	(125)		
	1.86[si]	1.85							**1.87**[si]	1.89[si]						
	2.71[w]	2.77														

tetrahedral Ti clusters will undergo solvent exchange, depending on the binding strength of the solvent molecules in the surrounding medium. Thus, for the Ti(η^1-OOH) and Ti(η^1-O_2H_2) clusters, the solvent would be an integral part of the complex, providing stabilisation through hydrogen bonding to the peroxidic moiety, whereas for the Ti(η^2-OOH) cluster, the solvent would be just weakly coordinated to the metal centre. Since the choice of solvent is known to exert a strong influence upon the catalytic reaction kinetics and the hydrated Ti(η^1-OOH) and Ti(η^1-O_2H_2) complexes are calculated to be −21 and −43 kJ mol^{-1} lower in energy than the 6-coordinate Ti(η^2-OOH) cluster, we therefore predict that the hydrated Ti(η^1-OOH) or Ti(η^1-O_2H_2) complexes are most likely to be the *oxygen-donating* species in hydrogen peroxide doped titanosilicate oxidation catalysts.

We now present a comparison of all of the DFT optimised Ti–peroxo models considered thus far with an EXAFS analysis of a *tert*-butyl hydroperoxide (TBHP) exposed Ti↑MCM-41 catalyst.

TBHP/Ti↑MCM-41 EXAFS

Each of the species a–l (Fig. 4–6) were used as starting points for the refinement of the Ti K-edge EXAFS data of a Ti↑MCM-41 catalyst reacted with TBHP. Full multiple scattering calculations were performed for each of the 12 structures. In Table 1, we give the DFT calculated and EXAFS refined Ti–O and Ti–Si distances and Ti–O–Si and Ti–O–O bond angles, *R* factor and energies of formation for 5- and 6-coordinate Ti(η^2-peroxo) species a–f. Similarly, the DFT calculated and EXAFS refined selected geometrical parameters, *R* factors and energies of formation for 5- and 6-coordinate Ti(η^1-peroxo) species g–j are given in Table 2. Finally, selected BP86/DZVP calculated and EXAFS refined bond lengths and bond angles for the dehydrated and hydrated Ti(η^1-O_2H_2) complexes, identified by this work, are shown in Table 3. The '*R* factor' is a measure of how close a theoretical model is to the experimental data: the lower the value, the closer the 'fit'.

Table 1 shows that the 6-coordinate DFT calculated Ti(η^2-OOH) complex, species a, is in excellent agreement with the experimental data, with an *R* factor of 15.9. The respective Fourier transforms for theory and experiment for a 6-coordinate Ti(η^2-OOH) cluster are shown in Fig. 7. This finding is in good agreement with our theoretical prediction that 6-coordinate Ti(η^2-OOH) clusters are present in activated titanosilicates. Of particular interest is the observation that the 5-coordinate analogue of the Ti(η^2-OOH) complex, species b, compares unfavourably with the experimental data (*R* factor of 25.2, Fig. 7). Furthermore, again in close agreement with our DFT studies, analysis of the experimental data shows that both 5- and 6-coordinate Ti(η^2-O_2) radical and Ti(η^2-OO^-) anion complexes are not found in TBHP/Ti↑MCM-41 catalysts. Turning now to the η^1 species, Table 2 shows that only the 6-coordinate five-membered ring Ti(η^1-OOH) DFT

Table 3 BP86/DZVP calculated (in bold) and refined TBHP/Ti↑MCM-41 EXAFS parameters for model dehydrated and hydrated (*i.e.* in the presence of one molecule of water) Ti(η^1–O_2H_2) species as iolated in this work. $E_{formation} = E_{total}$(Ti–$\eta^1$($O_2H_2$) + other products) – E_{total}(tripodal Ti^{IV} cluster + H_2O_2 + 2H_2O). [si] Ti–OSi bond length. [w] The Ti–O bond distance measured is that of Ti to the O in the water molecule. [p] Ti–peroxide bond length

	Dehydrated								Hydrated							
Cluster	Ti–O distance/Å		Ti–Si distance/Å		Ti–O–Si (Ti–O–OH) angle/°		$E_{formation}$/kJ mol^{-1} (*R* factor)		Ti–O distance/Å		Ti–Si distance/Å		Ti–O–Si (Ti–O–OH) angle/°		$E_{formation}$/kJ mol^{-1} (*R* factor)	
Ti–η'(O_2H_2)	**1.89**	1.90	**3.45**	3.28	**155.5**	155	−42		**1.92**	1.90	**3.38**	3.21	**150.4**	140	−87	
	2.36[p]	2.40	**3.45**	3.50	**165.0**	158	(25.64)		**2.27**[p]	2.40	**3.45**	3.35	**159.9**	155	(25.26)	
(k)	**1.85**[si]	1.84[si]	**3.38**	3.21	**150.7**	139		(l)	**1.83**[si]	1.83[si]	**3.43**	3.38	**160.9**	158		
	1.81[si]	1.84[si]			**(118.2)**	(120)			**1.83**[si]	1.83[si]			**(112.7)**	(112)		
	1.81[si]	1.84[si]							**1.80**[si]	1.83[si]						
									3.67[w]	3.29						

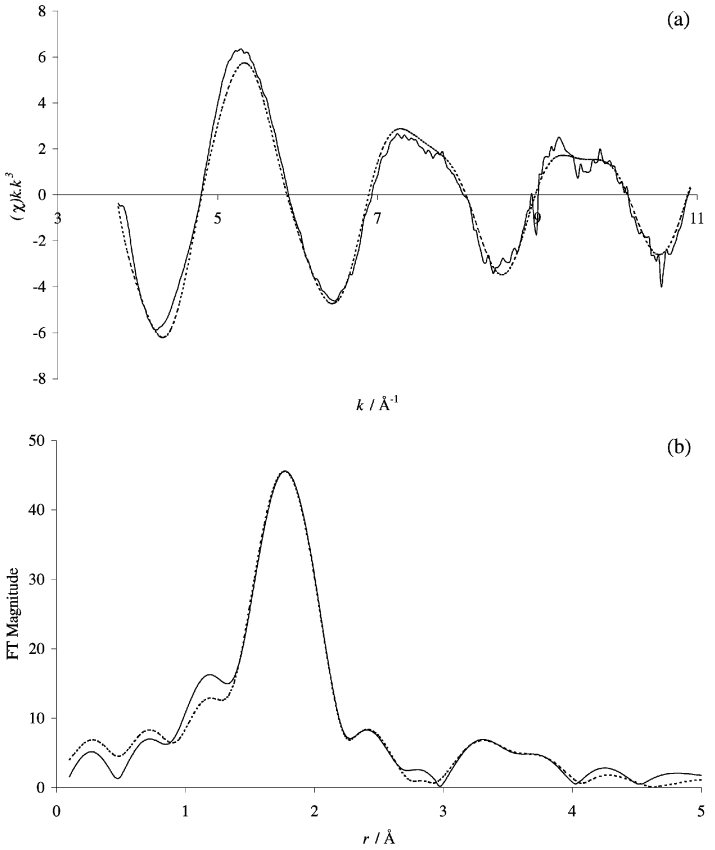

Fig. 7 Best EXAFS fit (a) and associated FT (b) for Ti↑MCM-41 catalyst employing the DFT optimised 6 coordinate Ti(η^2-OOH) cluster (species b, Fig. 4) as the starting model.

calculated model (species g, Fig. 5) agrees well with experiment, with an *R* factor of 15.8 (Fig. 7). Again, this observation is in good agreement with our theoretical predictions. Analysis of all the 5-coordinate species all resulted in a large discrepancy between the experimental and DFT calculated data or yielded unphysical structural parameters, in particular with regard to Debye–Waller factors and bond angles.

Table 3 presents the experimental and BP86/DZVP calculated geometrical parameters for the dehydrated and hydrated Ti(η^1-O_2H_2) complexes (Fig. 6), first identified in this work. Even though the formation of a dehydrated and hydrated Ti(η^1-O_2H_2) complex from the attack of H_2O_2 on a tetrahedral $(H_3SiO)_3$Ti–OH cluster was calculated to be energetically favourable, (−42 and −87 kJ mol^{-1}, respectively), we do not find good agreement of either model with experiment.

In order to achieve a more detailed comparison of our DFT calculated models with experiment we have calculated 5- and 6-coordinate Ti–peroxo species V and VI (Fig. 2) and dehydrated and hydrated Ti(η^1-O_2H_2) type complexes k and l (Fig. 6) employing TBHP as the peroxide. These six Ti–peroxo species were chosen since the ^{t}Bu group is an integral part of the complex, as shown in Table 4. BP86/DZVP optimisation of the Ti–peroxo species m–r, shown in Table 4, was performed and the resultant minimum energy structures were employed as the starting models for EXAFS refinement. The DFT calculated and experimentally refined bond angles, bond lengths, *R* factors and formation energies for species m–r are shown in Table 5. In agreement with our previous studies, with H_2O_2 as the sacrificial oxidant, both the hydrated (6-coordinate) Ti(η^2-OO^{t}Bu) and Ti(η^1-OO^{t}Bu) clusters are in good agreement with our EXAFS analysis of a TBHP/Ti↑MCM-41 catalyst, with *R* factors of 16.3 and 15.4 respectively. Again, even though our calculations suggest that the formation of species q and r is an energetically favourable process (with formation energies of −55 and −22 kJ mol^{-1}, respectively), we do not find any evidence in our experimental analysis for their presence in TBHP/Ti↑MCM-41 mixtures. Furthermore, it is surprising that there is little difference, both energetically as well as structurally, between the DFT calculated Ti–peroxo complexes considered when employing the computationally expensive TBHP as the sacrificial oxidant and those using H_2O_2.

Thus, X-ray absorption analysis of a TBHP exposed Ti↑MCM-41 catalyst confirms the formation of 6-coordinate Ti(η^1-OO^{t}Bu) and Ti(η^2-OO^{t}Bu) complexes, in agreement with our theoretical predictions.

Finally, in order to verify that the constraints imposed throughout this work on the second coordination shell Si ions do not affect our comparison of the DFT calculated models with experiment, we have calculated the 6-coordinate Ti(η^1-OOR) and Ti(η^2-OOR) complexes (where R = H) observed by experiment using a larger cluster size, extending to the third coordination shell from the central metal ion. Only two of the complexes considered were re-optimised with an extended cluster size due to the computationally demanding nature of the calculations involved. The BP86/DNP optimised 'extended' 6-coordinate Ti(η^1-OOH) and Ti(η^2-OOH) were used as the starting models for refinement of the EXAFS data. Both the BP86/DNP calculated and experimentally refined bond lengths and angles, *R* factors and formation energies are shown in Table 6. Examination of this Table 6 shows that there is minimal change in the structure or fit to experiment when employing the extended cluster model compared with the more computationally efficient clusters, which encompass just the first two coordination spheres around the central Ti ion.

Conclusion

In this paper we have probed, computationally, the structures and energetics of a range of possible oxygen-donating species

Table 4 Reaction schemes used to model the formation of hydrated and dehydrated Ti–peroxo complexes from the attack of TBHP on an $(H_3SiO)_3TiOH$ cluster

Hydrated	Dehydrated
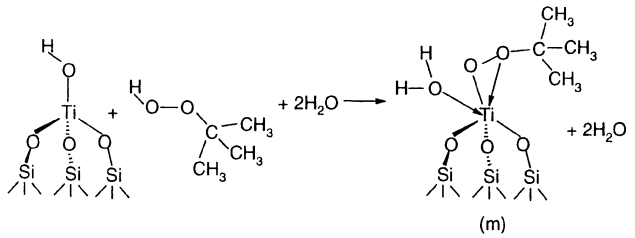 (m)	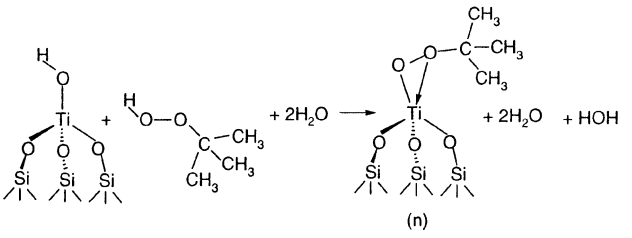 (n)
11 $(Ti–OH + HOO^tBu + 2H_2O \rightarrow Ti(\eta^2–OO^tBu) + 3H_2O$	12 $Ti–OH + HOO^tBu + 2H_2O \rightarrow Ti(\eta^2–OO^tBu)\cdot H_2O + 2H_2O$
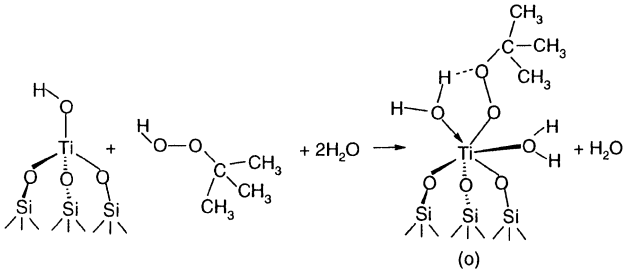 (o)	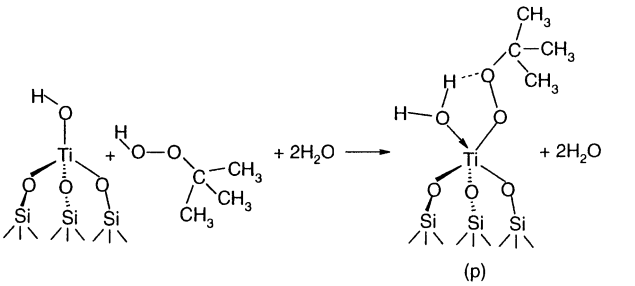 (p)
13 $Ti–OH + HOO^tBu + 2H_2O \rightarrow Ti(\eta^1–OO^tBu)(O(H)H) + 2H_2O$	14 $Ti–OH + HOO^tBu + 2H_2O \rightarrow Ti(\eta^1–OO^tBu)(O(H)H)\cdot H_2O + H_2O$
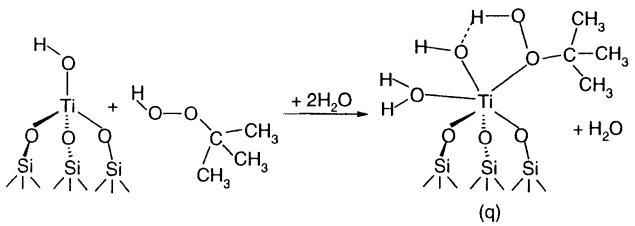 (q)	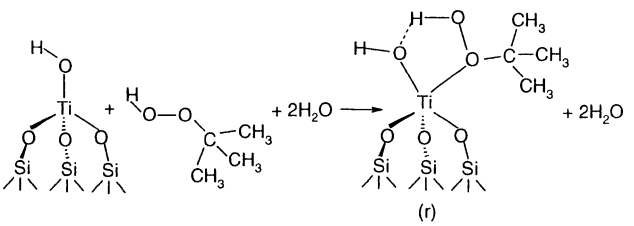 (r)
15 $Ti–OH + HOO^tBu + 2H_2O \rightarrow Ti(\eta^1–O^tBuOH)(OH) + 2H_2O$	16 $Ti–OH + HOO^tBu + 2H_2O \rightarrow Ti(\eta^1–O^tBuOH)(OH)\cdot H_2O + H_2O$

Table 5 BP86/DZVP calculated (in bold) geometrical parameters and formation energy for selected Ti–peroxo species arising from the attack of TBHP on a 2 C.S. bare Ti^{IV} site compared with the EXAFS refinement of a TBHP/Ti$^{\uparrow}$ MCM-41 catalyst (in standard font). $E_{formation} = E_{total}$(Ti–peroxo + other products) $- E_{total}$(tripodal Ti^{IV} cluster + TBHP + $2H_2O$). [si] Ti–OSi bond length. [w] The Ti–O bond distance measured is that of Ti to the O in the water molecule. [p] Ti–peroxide bond length

	Hydrated								Dehydrated							
Cluster	Ti–O distance/Å		Ti–Si distance/Å		Ti–O–Si (Ti–O–O^{t}Bu) angle/°		$E_{formation}$/kJ mol^{-1} (R factor)		Ti–O distance/Å		Ti–Si distance/Å		Ti–O–Si (Ti–O–O^{t}Bu) angle/°		$E_{formation}$/kJ mol^{-1} (R factor)	
	1.93[p]	1.98	**3.32**	3.33	**142.6**	151	**−39**		**1.89**[p]	1.95	**3.30**	3.22	**140.1**	139	**−16**	
Ti–η^2(OO^{t}Bu)	**2.24**[p]	2.21	**3.30**	3.24	**139.8**	141	(16.3)		**2.21**[p]	2.23	**3.42**	3.37	**157.9**	158	(28.03)	
	1.82[si]	1.84[si]	**3.45**	3.40	**159.7**	162			**1.84**[si]	1.83[si]	**3.36**	3.33	**148.7**	154		
(m)	**1.84**[si]	1.84[si]		(80.5)		(104)		(n)	**1.81**[si]	1.83[si]			**80.7**	(79)		
	1.84[si]	1.84[si]							**1.82**[si]	1.83[si]						
	2.48[w]	2.45														
	2.24	2.20	**3.35**	3.25	**146.6**	155	**−73**		**2.20**	2.17	**3.42**	3.41	**156.0**	162	**−46**	
Ti–η^1(OO^{t}Bu)	**1.97**[p]	1.93	**3.38**	3.35	**141.7**	142	(15.41)		**1.94**[p]	1.94	**3.38**	3.32	**146.2**	137	(20.3)	
	1.83[si]	1.83[si]	**3.42**	3.39	**160.0**	161			**1.82**[si]	1.85[si]	**3.36**	3.22	**148.2**	124		
(o)	**1.91**[si]	1.83[si]			**(116.6)**	(117)		(p)	**1.86**[si]	1.85[si]			**(122.6)**	(124)		
	1.82[si]	1.83[si]							**1.82**[si]	1.85[si]						
	2.34[w]	2.43														
	1.84	1.87	**3.27**	3.28	**136.1**	137	**−55**		**1.86**	1.89	**3.36**	3.24	**148.9**	139	**−22**	
Ti–η^1(O$_2$H^{t}Bu)	**3.22**[p]	3.06	**3.47**	3.40	**167.4**	161	(23.23)		**3.19**[p]	3.24	**3.46**	3.39	**168.2**	165	(25.61)	
	1.85[si]	1.84[si]	**3.44**	3.39	**163.8**	160			**1.81**[si]	1.83[si]	**3.38**	3.28	**152.0**	143		
(q)	**1.82**[si]	1.84[si]			**(77)**	(67)		(r)	**1.80**[si]	1.83[si]			**(100.2)**	(101)		
	1.79[si]	1.84[si]							**1.81**[si]	1.83[si]						
	3.15[w]	3.28														

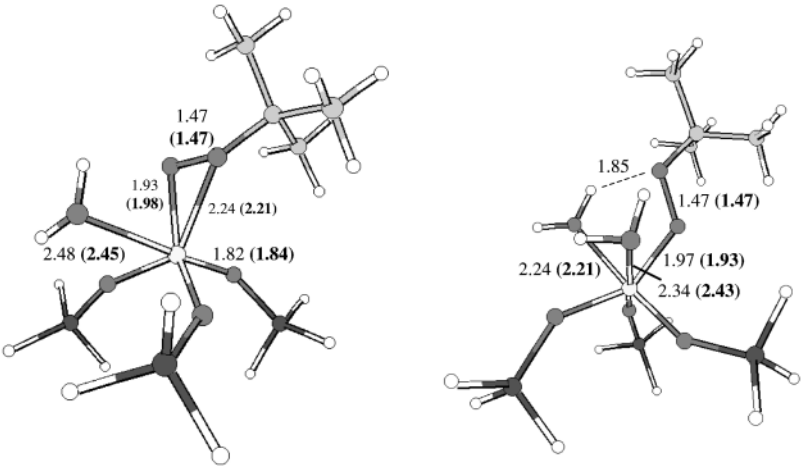

Scheme 1 Proposed Ti–peroxo species in TBHP/Ti↑MCM-41 catalysts. All distances shown are in Å, with experimental values highlighted in bold type and DFT calculated parameters in normal font.

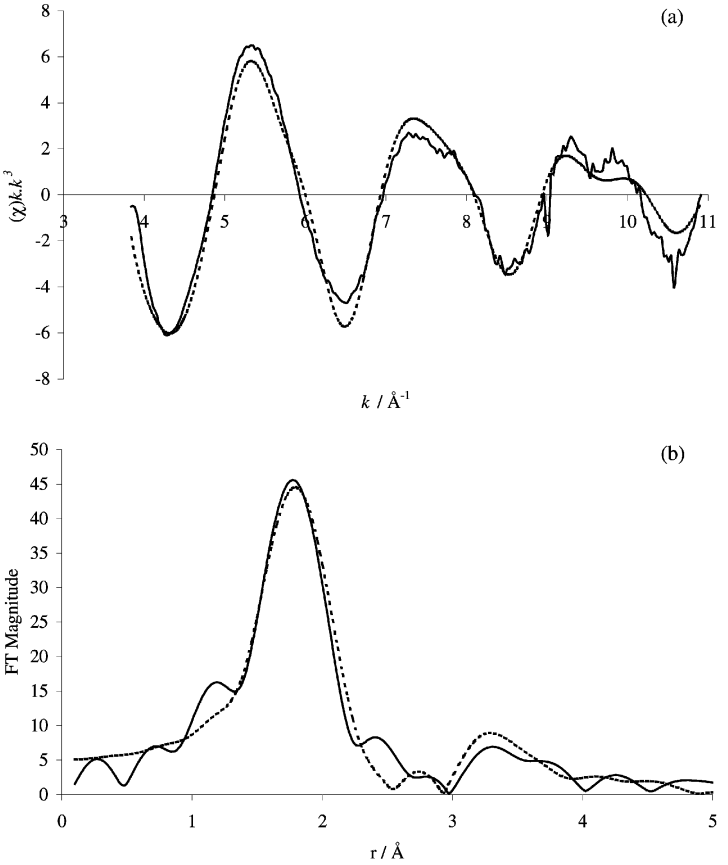

Fig. 8 Best EXAFS fit (a) and associated FT (b) for Ti↑MCM-41 catalyst employing the DFT optimised 5 coordinate Ti(η^2-OOH) cluster (species a, Fig. 4) as the starting model.

in surface grafted, Ti↑MCM-41 exposed to peroxide. The geometric parameters of these stationary point structures have been used as starting points for refinement of the Ti K-edge EXAFS data obtained from Ti↑MCM-41 exposed TBHP. Comparison of theory with experiment clearly indicates that the oxygen-donating species is 6-coordinate, with both η^2 (species a, Fig. 4) and η^1 (species g, Fig. 5) providing equally good fits to the EXAFS data. Scheme 1 shows selected theoretical and experimental parameters of η^1-OO^{t}Bu and η^2-OO^{t}Bu complexes postulated to exist in TBHP/Ti↑MCM-41 systems. Both 5- and 6-coordinate (*i.e.* dehydrated and hydrated) η^2-O_2, η^2-OO^- and η^1-OO^- type species are ruled out by the present study. Previously unidentified Ti(η^1-O_2H_2) type complexes (species k and l, Fig. 6) have been located computationally and are found to be stable with respect to the catalytic reactants. Although these species did not fit the experimental data well, this may be because coordination of water has not yet been included in the model. Thus, further work is needed to model this new complex in the presence of more than one molecule of water.

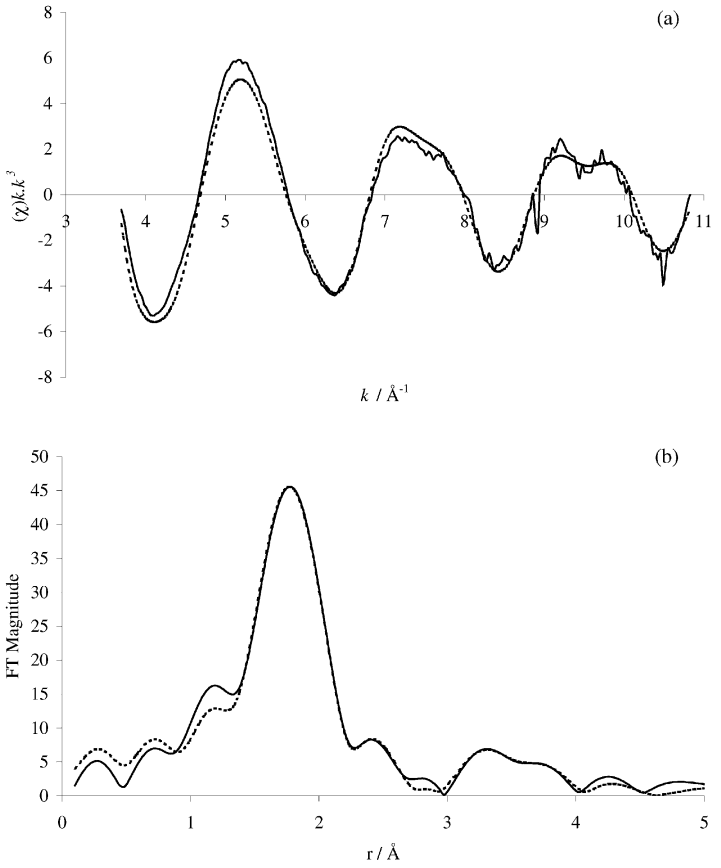

Fig. 9 Best EXAFS fit (a) and associated FT (b) for Ti↑MCM-41 catalyst employing the DFT optimised 6 coordinate Ti(η^1-OOH) cluster (species h, Fig. 5) as the starting model.

Table 6 BP86/DNP calculated (in bold) and refined TBHP/Ti↑ MCM-41 EXAFS parameters for 6-coordinate Ti(η^1-OOH) and Ti(η^2-OOH) 'extended' or 3 C. S. models. $E_{formation} = E_{total}$('extended' Ti–$\eta^1$(peroxo) + other products) – E_{total}('extended' tripodal Ti^{IV} cluster + H_2O_2 + $2H_2O$). [si] Ti–OSi bond length. [w] The Ti–O bond distance measured is that of Ti to the O in the water molecule. [P] Ti–peroxide bond length

Cluster	Ti–O distance/ Å		Ti–Si distance/ Å		Ti–O–Si (Ti–O–OH) angle/°		$E_{formation}$/ kJ mol^{-1} (R factor)
Ti–η^2(OOH)	**1.92**	1.91	**3.35**	3.38	**151.3**	160	**–45**
	2.25[P]	2.20	**3.32**	3.30	**145.5**	148	(16.02)
	1.83[si]	1.83[si]	**3.28**	3.21	**143.0**	139	
	1.80[si]	1.83[si]			**(81.9)**	(80)	
	1.80[si]	1.83[si]					
	2.26[w]	2.43					
Ti–η^1(OOH)	**2.24**	2.20	**3.31**	3.28	**145.3**	144	**–102**
	1.97[P]	1.97	**3.34**	3.38	**146.8**	152	(16.18)
	1.81[si]	1.83[si]	**3.34**	3.39	**151.5**	163	
	1.84[si]	1.83[si]			**(117.3)**	(120)	
	1.81[si]	1.83[si]					
	2.35[w]	2.43					

The present work illustrates again the power of our combination of theory with experiment in elucidating the three-dimensional structure of active sites in catalytic systems.

Acknowledgements

We thank EPSRC for financial support and CCLRC for computing facilities and beamtime. G.S. thanks the Leverhulme trust for a senior research fellowship. We are grateful to Accelrys for the provision of the DMOL and visualisation software.

References

1 B. Notari, *Adv. Catal.*, 1996, **41**, 253.
2 I. W. C. E. Arends, R. A. Sheldon, M. Wallau and U. Schuchardt, *Angew. Chem. Int. Ed. Engl.*, 1997, **36**, 1144.
3 M. Taramasso, B. Notari and G. Perego, *US Pat.* 4410501, (1983).
4 M. A. Camblor, A. Corma and J. Perezpariente, *Zeolites*, 1993, **13**, 82.
5 G. Sankar, F. Rey, J. M. Thomas, G. N. Greaves, A. Corma, B. R. Dobson and A. J. Dent, *J. Chem. Soc., Chem. Commun.*, 1994, 2279.
6 T. Maschmeyer, F. Rey, G. Sankar and J. M. Thomas, *Nature (London)*, 1995, **378**, 159.
7 T. Blasco, M. A. Camblor, A. Corma and J. Perezpariente, *J. Am. Chem. Soc.*, 1993, **115**, 11 806.
8 C. Lamberti, S. Bordiga, A. Zecchina, G. Vlaic, G. Tozzola, G. Petrini and A. Carati, *J. Phys. IV*, 1997, **7**, 851.
9 C. Lamberti, S. Bordiga, D. Arduino, A. Zecchina, F. Geobaldo, G. Spano, F. Genoni, G. Petrini, A. Carati, F. Villain and G. Vlaic, *J. Phys. Chem. B*, 1998, **102**, 6382.
10 R. D. Oldroyd, G. Sankar, J. M. Thomas and D. Ozkaya, *J. Phys. Chem. B*, 1998, **102**, 1849.
11 D. Gleeson, G. Sankar, C. R. A. Catlow, J. M. Thomas, G. Spano, S. Bordiga, A. Zecchina and C. Lamberti, *Phys. Chem. Chem. Phys.*, 2000, **2**, 4812.
12 G. Sankar, J. M. Thomas and C. R. A. Catlow, *Top. Catal.*, 2000, **10**, 255.
13 S. Bordiga, S. Coluccia, C. Lamberti, L. Marchese, A. Zecchina, F. Boscherini, F. Buffa, F. Genoni, G. Leofanti, G. Petrini and G. Vlaic, *J. Phys. Chem.*, 1994, **98**, 4125.
14 T. Tatsumi, K. Yanagisawa, K. Asano, M. Nakamura and H. Tominaga, *Zeolite Microporous Crystals*, 1994, **83**, 417.
15 F. Geobaldo, S. Bordiga, A. Zecchina, E. Giamello, G. Leofanti and G. Petrini, *Catal. Lett.*, 1992, **16**, 109.

16 L. Marchese, T. Maschmeyer, E. Gianotti, S. Coluccia and J. M. Thomas, *J. Phys. Chem. B*, 1997, **101**, 8836.
17 G. N. Vayssilov and R. A. van Santen, *J. Catal.*, 1998, **175**, 170.
18 A. Jentys and C. R. A. Catlow, *Catal. Lett.*, 1993, **22**, 251.
19 P. E. Sinclair, G. Sankar, C. R. A. Catlow, J. M. Thomas and T. Maschmeyer, *J. Phys. Chem. B*, 1997, **101**, 4232.
20 A. Jentys, G. Warecka, M. Derewinski and J. A. Lercher, *J. Phys. Chem.*, 1989, **93**, 4837.
21 A. de Man and J. Sauer, *J. Phys. Chem.*, 1996, **100**, 5025.
22 G. Tozzola, M. A. Mantegazza, G. Ranghino, G. Petrini, S. Bordiga, G. Ricchiardi, C. Lamberti, R. Zulian and A. Zecchina, *J. Catal.*, 1998, **179**, 64.
23 G. Ricchiardi, A. de Man and J. Sauer, *Phys. Chem. Chem. Phys.*, 2000, **2**, 2195.
24 J. M. Thomas and G. N. Greaves, *Science*, 1994, **265**, 1675.
25 P. E. Sinclair and C. R. A. Catlow, *J. Chem. Soc., Chem. Commun.*, 1997, 1881.
26 B. Notari, *Catal. Today*, 1993, **18**, 163.
27 M. G. Clerici, *Appl. Catal.*, 1991, **68**, 249.
28 P. E. Sinclair and C. R. A. Catlow, *J. Phys. Chem. B*, 1999, **103**, 1084.
29 R. D. Oldroyd, J. M. Thomas, T. Maschmeyer, P. A. MacFaul, D. W. Snelgrove, K. U. Ingold and D. D. M. Wayner, *Angew. Chem. Int. Ed. Engl.*, 1996, **35**, 2787.
30 D. R. C. Huybrechts, P. L. Buskens and P. A. Jacobs, *J. Mol. Catal.*, 1992, **71**, 129.
31 D. R. C. Huybrechts, I. Vaesen, H. X. Li and P. A. Jacobs, *Catal. Lett.*, 1991, **8**, 237.
32 E. Karlsen and K. Schoffel, *Catal. Today*, 1996, **32**, 107.
33 P. E. Sinclair, PhD Thesis, University of London, 1997.
34 N. Jappar, Q. H. Xia and T. Tatsumi, *J. Catal.*, 1998, **180**, 132.
35 C. B. Khouw, C. B. Dartt, J. A. Labinger and M. E. Davis, *J. Catal.*, 1994, **149**, 195.
36 K. U. Ingold, D. W. Snelgrove, P. A. MacFaul, R. D. Oldroyd and J. M. Thomas, *Catal. Lett.*, 1997, **48**, 21.
37 M. G. Clerici, G. Bellussi and U. Romano, *J. Catal.*, 1991, **129**, 159.
38 M. G. Clerici and P. Ingallina, *J. Catal.*, 1993, **140**, 71.
39 A. Bhaumik, P. Kumar and R. Kumar, *Catal. Lett.*, 1996, **40**, 47.
40 K. A. Jorgensen, *J. Chem. Soc., Perkin Trans. 2*, 1994, 117.
41 A. Corma, P. Esteve and A. Martinez, *J. Catal.*, 1996, **161**, 11.
42 T. Sato, J. Dakka and R. A. Sheldon, *Zeolites Related Microporous Mater.*, 1994, **84**, 1853.
43 G. F. Thiele and E. Roland, *J. Mol. Catal. A.*, 1997, **117**, 351.
44 M. Neurock and L. E. Manzer, *J. Chem. Soc., Chem. Commun.*, 1996, 1133.
45 G. Bellussi, A. Carati, M. G. Clerici, G. Maddinelli and R. Millini, *J. Catal.*, 1992, **133**, 220.
46 The Pure DFT code Dgauss[4.1], Oxford Molecular Inc.
47 Unichem[4.1], Oxford Molecular Inc.
48 S. P. Greatbanks, I. H. Hillier, N. A. Burton and P. Sherwood, *J. Chem. Phys.*, 1996, **105**, 3770.
49 A. Becke, *Phys. Rev. A*, 1988, **38**, 3098.
50 J. Perdew and Y. Wang, *Phys. Rev. B*, 1986, **33**, 8800.
51 M. Nusair, L. Wilk and S. H. Vosko, *J. Phys. F.*, 1981, **11**, 1683.
52 L. Wilk, M. Nusair and S. H. Vosko, *Can. J. Phys.*, 1981, **59**, 585.
53 Dmol[4.2], Molecular Simulations Inc.
54 Cerius[2], Molecular Simulations Inc.
55 P. A. Barrett, G. Sankar, C. R. A. Catlow and J. M. Thomas, *J. Phys. Chem.*, 1996, **100**, 8977.